Oxygen contribution to the magnetic response of ultrathin Fe/Ni multilayers grown on Fe-*p*(1×1)O

F. Goto[1], G. Perozzi[1], A. Calloni[1,*], G. Albani[1], G. Fratesi[2], S. Achilli[2], L. Duò[1], M. Finazzi[1], F. Ciccacci[1] and G. Bussetti[1]

[1]*Dipartimento di Fisica, Politecnico di Milano, Piazza Leonardo Da Vinci, 32, 20133 Milano, Italy*
[2]*ETSF and Dipartimento di Fisica "Aldo Pontremoli", Università degli Studi di Milano, Via Celoria, 16, 20133 Milano, Italy*
*alberto.calloni@polimi.it

Abstract
We investigated the magnetic behaviour of an Fe overlayer on a Ni buffer layer (Fe/Ni multilayer system) grown on top of the Fe-*p*(1×1)O surface, with a particular focus on the modifications observed in the spin-resolved electronic structure and the role of oxygen, introduced in the system in a well-defined amount at the substrate preparation stage. The structural properties are investigated by means of low energy electron diffraction, that confirms the formation of an epitaxial system featuring a metastable surface lattice. Spin-resolved photoemission spectroscopy testifies a strong decrease of the spectral spin polarization for increasing thickness of the Ni buffer layer, reaching a minimum from a nominal thickness of 6 Ni atomic layers. Surprisingly, the growth of a single Fe overlayer is sufficient to restore most of the original polarization signal, thus creating an ultrathin *bcc* Fe film seemingly decoupled from the substrate. *Ab initio* calculations track the modifications of the magnetic moments of the surface layers that quench upon Ni deposition and restore with additional Fe growth. Spin-resolved inverse photoemission highlights a notable reduction of the density of majority states just above the Fermi level, possibly influencing the magnetic response of the system.

Introduction
The growth of Fe/Ni heterostructures offers the unique possibility of stabilizing unusual crystallographic phases, characterized by novel electronic and magnetic properties [1]. From a fundamental point of view, the investigation of such systems aims at (i) elucidating the physics which comes into play during the formation of hetero-interfaces and ultra-thin films and (ii) linking the structural and electronic properties to the magnetic response of such complex systems in terms, *e.g.*, of their magnetic coercivity and anisotropy [2]. The study of metastable crystallographic phases, with reduced dimensionality, of known magnetic materials (like Fe and Ni) can give a contribution to the understanding of the physics that rules the magnetic behaviour at the surface of a highly interacting magnetic material. From the point of view of applications, magnetic Fe(Ni) nanostructures and metastable systems with novel magnetic phases are expected to rival the performances of more expensive rare earths-containing materials [3].

Previous literature investigations have studied *bcc* Ni films grown on low-interacting, non-magnetic substrates like GaAs(001) [4], or magnetic substrates such as Fe(001) to form a magnetically coupled interface with the magnetization of the film strongly affected by the substrate contribution [5]. Fe/Ni exchange-coupled multilayers grown on non-magnetic substrates such as Ag(001) or Cu(001), are also reported [6,7]. In the present work, the Fe(001) substrate is treated in order to form an oxygen-rich superstructure, namely the Fe-*p*(1×1)O surface. Generally, an oxygen overlayer has a surfactant effect since it tends to float on the growing film and lowers the kinetic barriers for adatom diffusion [6,7]. This behaviour can be exploited in homo and hetero-epitaxial growth to improve the smoothness of surfaces and interfaces [8]. In the particular case of Ni on Fe-*p*(1×1)O, however, we demonstrated a peculiar morphological evolution where oxygen increases the roughness of the surface (anti-surfactant effect) at few

monolayer (ML) coverage [9,10]. Additionally, in metastable systems oxygen is known to intervene in the process of structural relaxation [11] and, in general, to influence the magnetic behaviour at the surface and at heterointerfaces [12,13].

In this frame, we focused on the magnetic response of the Fe overlayer placed on a Ni buffer layer, the latter grown on the Fe-*p*(1×1)O system, by the combined use of spin-polarized ultraviolet photoemission (SP-UPS) and inverse photoemission (SP-IPES) spectroscopies. As Ni is deposited on the Fe-*p*(1×1)O substrate, a strong decrease of the spin-polarization signal associated to specific surface features is observed, indicating a quenching of the surface magnetization. The evolution of the spectral spin-polarization is then studied for a Fe overlayer deposited on a 6 ML Ni/Fe-*p*(1×1)O. We observe a sudden restoration of the spin polarization in the band structure by depositing only a single Fe ML on the Ni buffer layer. For empty states, we record the same re-activation of the overall spectral spin polarization, with the notable quenching of a majority feature located immediately above the Fermi level. For all the samples there were no signs of surface relaxation of Ni towards the thermodynamically stable *fcc* phase, as testified by low energy electron diffraction (LEED). This observation suggests the possibility of applying our method to the growth of metastable Fe/Ni multilayers with little or no structural evolution. As a further confirmation of this general picture, we ran complementary *ab-initio* simulations based on density functional theory (DFT) and a simplified model featuring an epitaxial multilayer film with atomically sharp interfaces. The simulation reproduces the general behaviour of the polarization signal and provides a rationale to link it to the evolution of the surface magnetization.

Experimental

The sample is prepared in UHV conditions ($p_{\mathrm{base}} \approx 1 \times 10^{-8}\ \mathrm{Pa}$) and characterized *in-situ* by LEED, X-rays photoemission spectroscopy (XPS) and spin-resolved photoemission and inverse photoemission spectroscopies in the UV range. A detailed description of the experimental apparatus can be found in Ref. [14]. The substrate is a 500 nm thick Fe layer deposited on MgO(001) by molecular beam epitaxy (MBE). Starting from clean *bcc* Fe(001), the Fe-*p*(1×1)O surface is obtained by exposing the substrate, held at 720 K, to 30 L of oxygen ($1\mathrm{L} = 1.33 \times 10^{-4}\ \mathrm{Pa}\cdot\mathrm{s}$), and flashing the sample at 970 K to desorb the oxygen in excess [12]. Nickel (Iron) is evaporated by electron bombardment of a Ni (Fe) rod. The thickness of one nickel (iron) monolayer is $1\ \mathrm{ML_{Ni}} = 1.33\ \text{Å}$ ($1\ \mathrm{ML_{Fe}} = 1.43\ \text{Å}$) [15]. The evaporation rate (approximately $0.6\ \text{Å}\ \mathrm{min}^{-1}$) is measured by a quartz crystal microbalance and the final coverage is determined by the substrate exposure time to the molecular beam. In this work, all the film coverages are reported in nominal thicknesses. The deposition was performed at room temperature to minimize Fe/Ni interdiffusion [10]. Cycles of Ar^+ ion sputtering ($E_{\mathrm{beam}} = 1500$ eV, $I_{Ar+} = 2.5$ μA) and annealing at 750 K are used to recover a clean *bcc* Fe substrate.

The growth process is studied by means of XPS performed with a non-monochromatic $\mathrm{Mg\ K}\alpha$ source ($h\nu = 1253.6\ \mathrm{eV}$). The valence band at normal emission is studied performing *in situ* SP-UPS. Spectra are obtained using a HeI photon source ($h\nu = 21.2\ \mathrm{eV}$) and photoelectrons are collected by a 150 mm hemispherical analyser combined with a Mott detector, to get access to the in-plane spin polarization of the electronic band structure. The Sherman function of the detector is $S = 0.14$ [14]. SP-UPS measurements are performed at magnetic remanence on samples previously magnetized by sending a current pulse through a coil, thus generating a peak magnetic field of $1000\ \mathrm{Oe}$ along two opposite directions of the Fe(001) substrate ([100] and $[\bar{1}00]$). Both magnetization directions are investigated to remove experimental asymmetries from the SP-UPS spectra, as explained in Ref. [16]. The energy levels above the Fermi level, *i.e.*, unoccupied electronic states, are probed *in situ* by spin polarized inverse photoemission spectroscopy, performed using a GaAs photocathode as electron source and detecting $9.6\ \mathrm{eV}$ photons with a band pass detector (isochromatic mode) [14]. The full width at half maximum resolution of XPS is about 1 eV, while for SP-UPS and SP-IPES experiments is about 150 and 700 meV, respectively.

Theory

The theoretical analysis is based on first-principle density functional theory (DFT) simulations within the generalized gradient approximation for the exchange and correlation functional in the form proposed by Perdew, Burke and Ernzerhof (GGA-PBE) [17]. We considered a model featuring homogeneous and commensurate Ni and Fe layers with a *p*(1 × 1)O superstructure on top of *bcc* Fe. Such a system is modelled by a slab with a total of 25 metal layers, the bottom 13 fixed to their bulk positions, and O as a top layer. Slabs are periodically repeated with a vacuum portion of 22 Å. We adopt the Quantum-ESPRESSO simulation package [18,19] with plane waves and ultrasoft pseudopotentials. The latter, generated from scalar-relativistic all-electron atomic calculations, are taken from our previous work [20]. We sample the surface Brillouin zone by a 14×14 Monkhorst-Pack mesh.

Results and discussion

Growth studies and morphology

The results of XPS experiments, in the binding energy regions of Fe $2p_{3/2}$, Ni $2p_{3/2}$, and O $1s$ core levels, are shown in **Figure 1**.

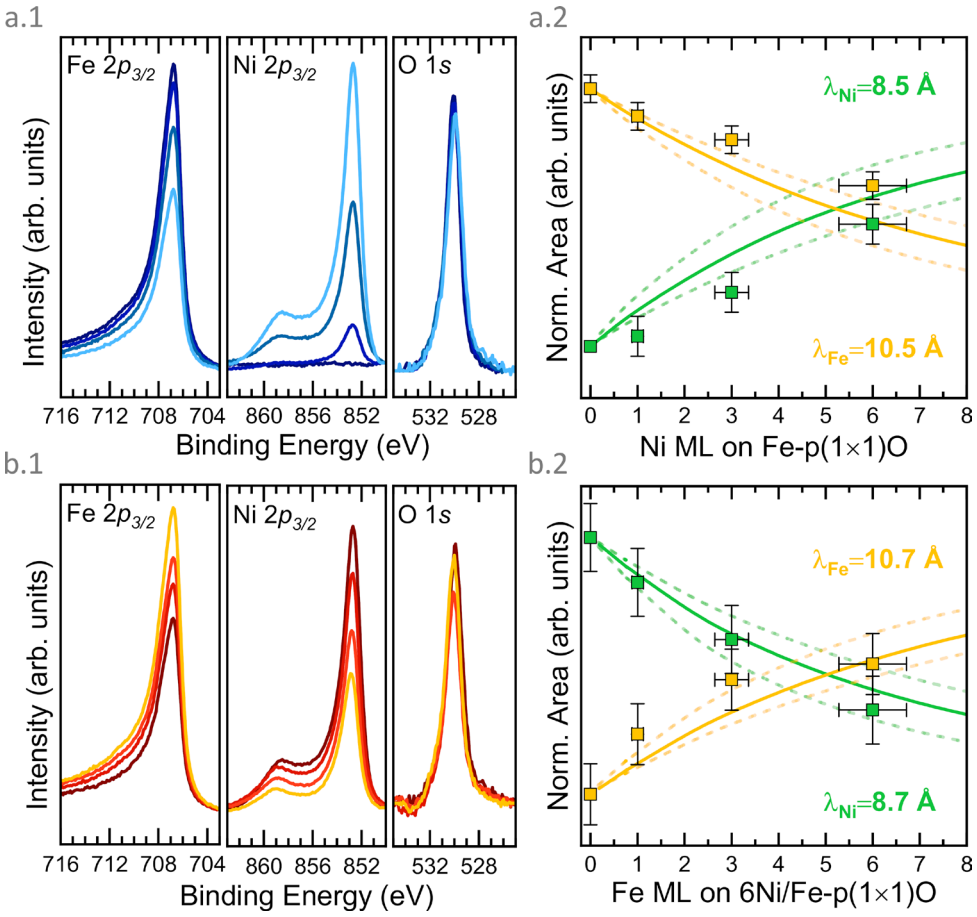

Figure 1: XPS spectra acquired in the Fe $2p_{3/2}$, Ni $2p_{3/2}$ and O 1s energy regions (a.1) for increasing Ni coverage on Fe-p(1×1)O substrate (blue series); (b.1) for increasing Fe coverage on 6 Ni/Fe-p(1×1)O (red series). A Shirley background has been subtracted from all the spectra. On the right the normalized area of Fe(Ni) peaks is plotted with yellow(green) symbols as function of the nominal Ni (panel a.2) or Fe (panel b.2) thickness. Continuous lines describe the exponential decay/enhancement of the photoemission signal assuming an uniform covering of the surface with Ni or Fe (dot lines account for the reported accuracy of the estimates regarding the photoelectron inelastic mean free path) [24].

Focusing on the growth of the Ni buffer layer (Figure 1a), we observe that the intensity of the O 1*s* signal is almost constant as the Ni thickness increases, confirming the fact that the oxygen layer floats to the sample surface during the growth [9]. The binding energy (BE) position of the O $1s$ peak is (529.9 ± 0.3) eV

considering all investigated samples, compatible with the presence of either Ni-O or Fe-O bonds {$BE = (529.7 \pm 0.3)$ eV and $\mathrm{BE} = (529.9 \pm 0.4)$ eV, respectively [21]}. The Ni $2p_{3/2}$ spectra are characterized by a main peak and a satellite structure at larger binding energies (about 6 eV), typical of metallic Ni [22]. No clear evidence is given of the typical features of oxidized nickel, in agreement with previous reports on chemisorbed O on Ni and Ni oxide phases obtained in oxygen-deficient environments [23], where the final peak position is distinctively different from that reported for the NiO bulk phase {about 854 eV [21]}. The normalized Fe $2p_{3/2}$ and Ni $2p_{3/2}$ peak area, determined at each growth step after background subtraction, is plotted in Figure 1a as a function of the nominal layer thickness. Continuous lines are exponential functions describing the attenuation/enhancement of the signal intensity in case of an uniform covering of the surface by a Ni layer of the reported nominal thicknesses. The inelastic mean free path for photoelectron is calculated for *bcc* Ni and Fe according to the TPP-2M model [24]. The attenuation of the iron signal is less pronounced than expected, possibly related to an increased surface roughness related to the aforementioned anti-surfactant effect of O and/or a partial Fe segregation through Ni [9,10].

A Ni film with a thickness of 6 ML was used as the starting layer for the subsequent Fe depositions, up to 6 ML of Fe (Figure 1b). The O 1*s* intensity is still high [≈90% of the signal characteristic of the Fe-*p*(1×1)O surface], confirming that oxygen is floating to the topmost layer. The intensity evolution of the Fe $2p_{3/2}$ and Ni $2p_{3/2}$ features is well described by the exponential growth model within our experimental errors, suggesting that Fe atoms progressively cover the Ni buffer layer.

In **Figure 2**, the Fe/Ni multilayer LEED characterization (b-column, in the centre) is presented together with a peak-intensity analysis (c-column, on the right) and a schematic multilayer structure (a-column, on the left), where interfaces are depicted sharp for a comparison with the developed theoretical model (see below).

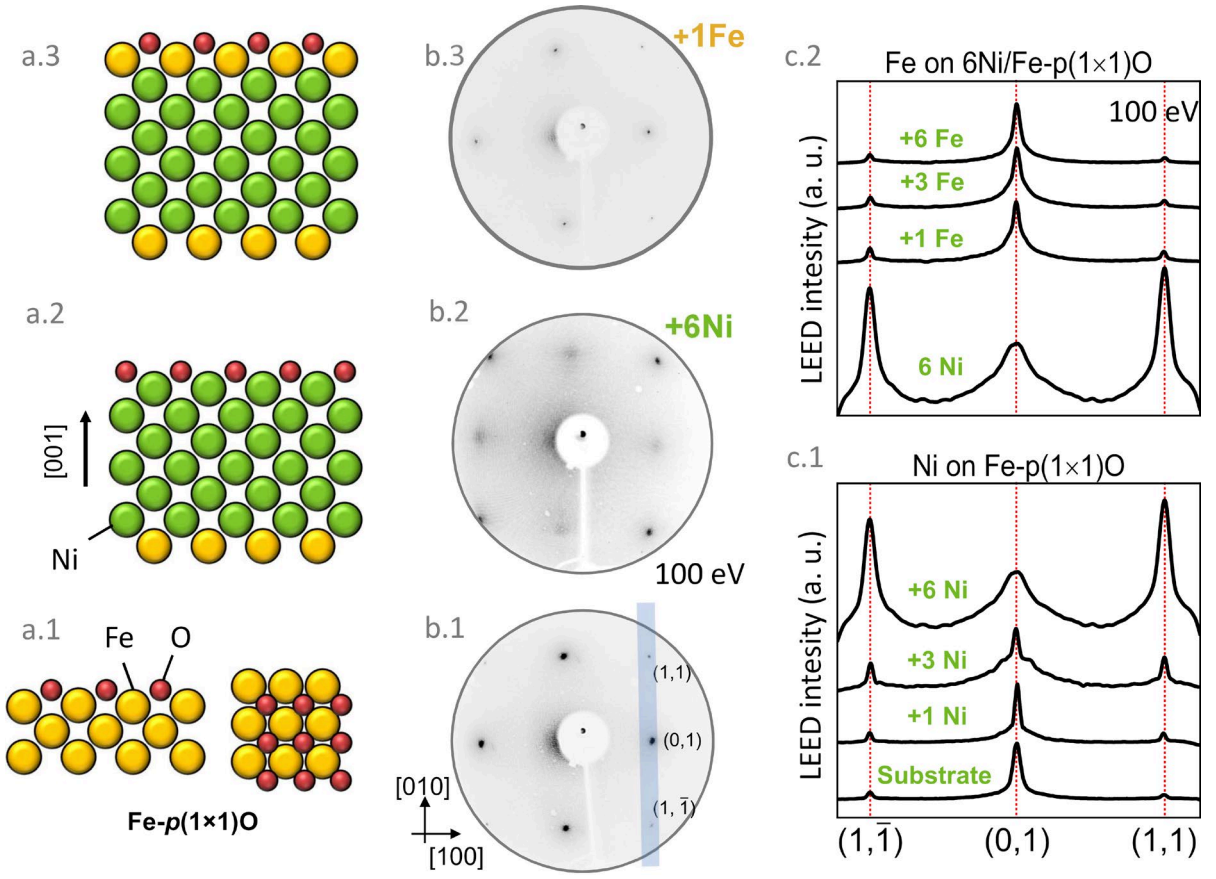

Figure 2: (a.1 ÷ a.3) schematic side view of the multilayer structure for selected Ni and Fe coverages; (b.1 ÷ b.3) corresponding LEED pictures; (c.1 and c.2) evolution of the LEED spot intensities upon the growth of the multilayer structure (see text for details).

Starting from the Fe-*p*(1×1)O substrate (Figures 2a.1 and 2b.1) up to 6 ML of Ni (Figures 2a.2 and 2b.2) and then for 1 ML of Fe on the 6 ML Ni/Fe-*p*(1×1)O buffer layer (Figures 2a.3 and 2b.3), the LEED square pattern of the *bcc* substrate is preserved. This means that the atoms of the buffer layer form a pseudomorphic square lattice, which remains stable after further depositions. This interpretation is strengthened by the LEED intensity spot analysis. In figure 2c the intensity profile of the LEED pattern along the $[010]$ direction is plotted for different samples and normalized with respect to the maximum of each curve to highlight relative intensity variations between the different LEED spots. Starting from the Fe-*p*(1×1)O substrate (bottom panel), as the coverage of Ni increases, the $(1,0)$ spot decreases its intensity and the $(1,1)$ spot becomes more evident. The subsequent deposition of Fe has the effect to enhance the $(1,0)$ spot, and lower again the $(1,1)$ one. In the end, a LEED pattern very close to that of the Fe-*p*(1×1)O substrate is observed. The evolution of the $(1,1)$ spot is directly linked to the growth sequence and confirms the restoration of the pristine surface lattice upon Fe dosing on the Ni buffer layer.

Spin Polarization Evolution of electronic states

SP-UPS and SP-IPES results for the Fe/Ni multilayer system are reported in **Figure 3**a.The green (red) lines represent the signal due to majority (minority) electrons, with their spin oriented along the in-plane magnetization direction. On the right, (Figure 3b) the spin polarization of selected energy regions (A,B,C,D) is reported for all the samples, normalized to the substrate polarization (P_{Meas}/P_{Sub}) to highlight the evolution of the spectral polarization with the multilayer thickness.

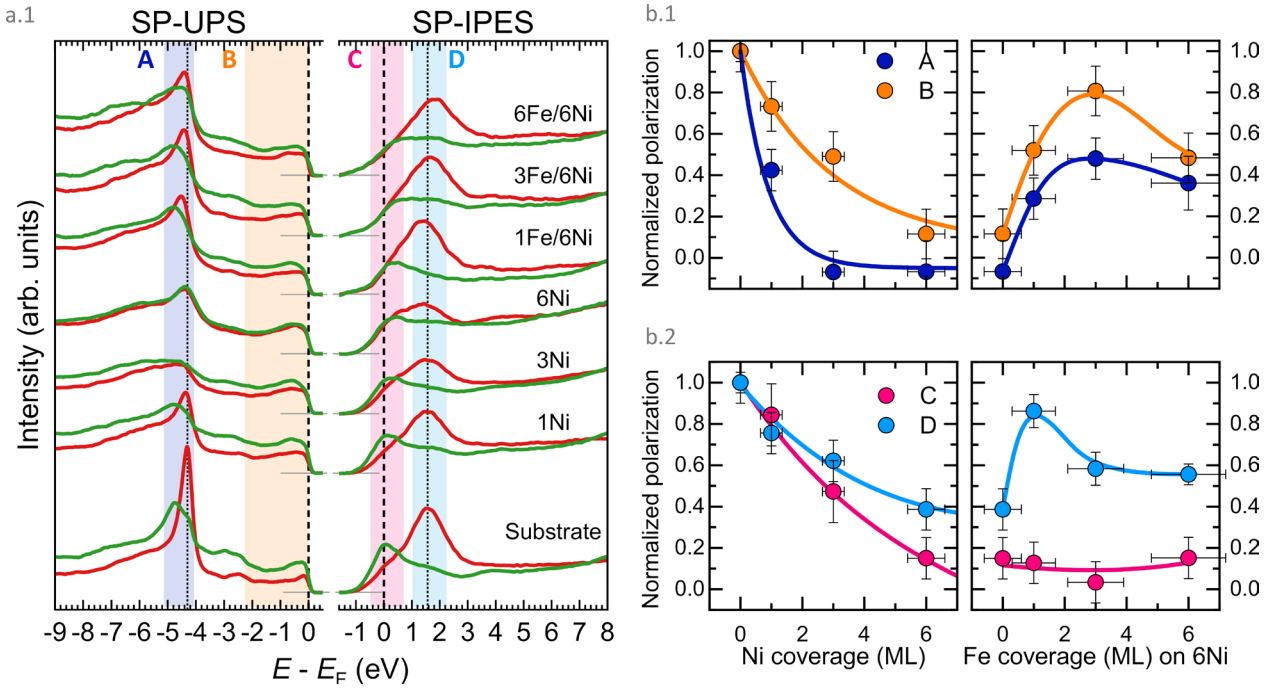

Figure 3: (a) SP-UPS and SP-IPES spectra at different coverages of the Ni buffer layer on top of the Fe-p(1×1)O substrate and Fe overlayer on the 6 Ni/Fe-p(1×1)O buffer layer. Green (red) lines are related to majority (minority) spin electrons. Normalized spin polarization (P_{Meas}/P_{Sub}) of occupied (b.1) and empty (b.2) states, related to the A-B and C-D energy regions, respectively, plotted as function of the Ni and Fe layer thickness. Lines are guides to the eye.

The Fe-*p*(1×1)O spectra, at the bottom of Figure 3a, is dominated by majority electrons below the Fermi level and minority electrons above, according to literature [14,25]. The spectroscopic fingerprint of the Fe-*p*(1 × 1)O substrate is the O 2*p* related state at about -4.5 eV (region A), mainly populated by minority electrons ($P \approx -25\%$). Above the Fermi energy (E_F), the IPES signal is dominated by two spin-polarized features (regions C, D) associated to bulk Fe states located along the $\bar{\Gamma}\bar{\mathrm{H}}$ direction of the Fe Brillouin zone [12,25].

The spectroscopic signal related to oxygen is present in all UPS spectra, confirming that oxygen atoms are always present at the sample surface. The presence of an oxygen feature at about -4.5 eV is therefore characteristic of both the substrate *p*(1 × 1)O superstructure and the oxygen-reconstructed surface of the Ni buffer layer, consistent with literature results dealing with O chemisorption on other *bcc* surfaces, such as those of Cr(001) [26] and 1ML Cr/Fe-*p*(1 × 1)O [27].

A complete quenching of the spin polarization is observed for the oxygen state (region A) upon the growth of Ni. A strong attenuation is observed also in the region B, where the polarization is reduced to some 10% of the value for the pristine Fe-*p*(1 × 1)O surface. For empty states we see a similar behaviour immediately above the Fermi level (region C, $P_C \approx 15\%$), while the attenuation is less intense for the minority channel (region D) with a final polarization $P_D \approx 40\%$. The strong attenuation of the spin polarization for filled electronic states can be compared with the results obtained when Ni is grown directly on the bare Fe(001) substrate {see, *e.g.*, the results of Ref. [5], obtained with a different photon source}. There, pseudomorphic *bcc* nickel was found ferromagnetic with a normalized spin polarization of $P \approx 25\% \pm 5\%$. The comparatively lower signal observed in our case suggests that the presence of oxygen reduces the magnetic response of the topmost Ni atoms, as also found in our model calculations (see below).

The evolution of the spectral spin polarization of the selected features is then studied when an Fe overlayer is deposited on the 6 ML Ni/Fe-*p*(1 × 1)O system (Figure 3b). At 1 ML coverage, a strong restoration of the spin polarization is observed for the oxygen peak (region A) as well as in the pre-Fermi region (B) and for the minority peak in empty states (region D). Such a restoration persists also for the 3 ML- and 6 ML-thick Fe overlayers. We note that the polarization of the IPES spectra related to region C is characterized by a different behaviour: the spin signal is always quenched also for the highest overlayer thickness explored, *i.e.*, 6 ML of iron on the 6 ML Ni buffer layer.

To better resolve the evolution of the spin-polarized spectra as a function of the buffer layer thickness, **Figure 4**a shows a comparison between SP-UPS and SP-IPES results of 1 ML of Fe on 6 Ni/Fe-*p*(1×1)O (bottom spectra) and a new multilayer system featuring a thicker Ni layer, namely 1 ML of Fe on 12 ML Ni/Fe-*p*(1×1)O (top spectra). The contribution of the buffer layer is plotted with light lines.

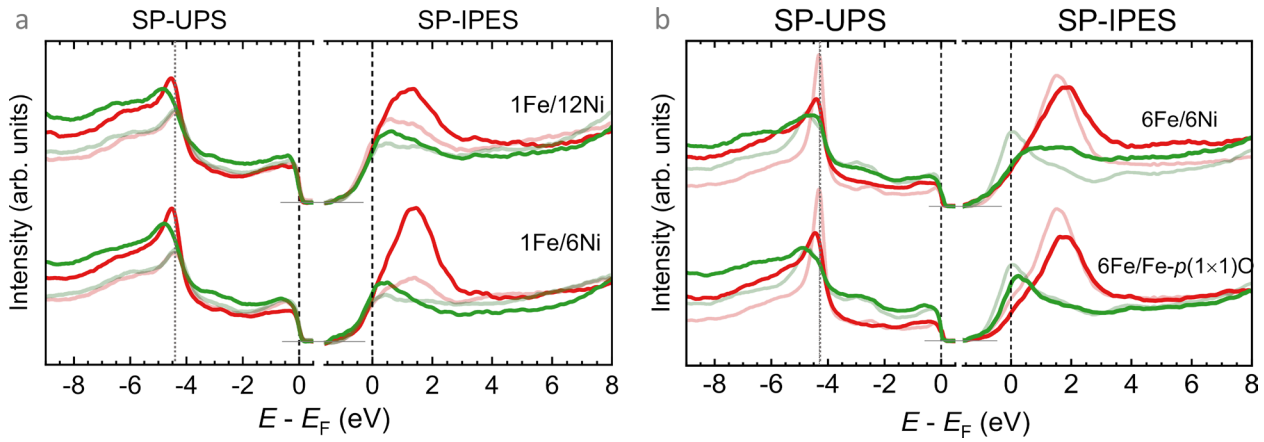

Figure 4: (a), SP-UPS and SP-IPES spectra of 1 ML of Fe on 6 Ni and 12 Ni buffer layers. Light curves are the spectra related to the buffer layer. (b) SP-UPS and SP-IPES spectra of 6 ML of Fe on 6 ML Ni buffer layer, compared with 6 ML of Fe directly grown on the Fe-p(1×1)O substrate. The Fe-p(1×1)O spectra are plotted with light colors, the position of the oxygen-related peak in SP-UPS is marked by a vertical dotted line.

Also for the thicker (12 ML) buffer layer, we observe a sharp restoration of the spin polarization signal suggesting that, within the explored multilayer systems, the restoration is independent from the distance between the Fe overlayer and the underlying (original) Fe-*p*(1×1)O substrate. The differences observed in the spectral lineshape can be related to the contribution from the photoemission features of the buffer layer (see, *e.g.*, the minority peak at 0.8 eV).

Figure 4b compares the photoemission spectra acquired from the 6 ML Fe/6 ML Ni/Fe-*p*(1×1)O system (top spectra) to the ones acquired in the case of Fe homoepitaxy on Fe-*p*(1×1)O (bottom spectra). In the SP-PES spectra, the oxygen related peak at around 4.5 eV below E_F (vertical dotted line in Figure 4) is less sharp with respect to the bare Fe-*p*(1×1)O surface (light lines), resulting in a reduced spin polarization. Such a broadening of the oxygen signal can be explained by an increased disorder of the oxygen layer as a result of either the oxygen segregation process or an increased morphological disorder due to the RT growth of the overlayers, resulting in slightly different O adsorption sites. In the case of SP-IPES spectra, we observe a slight reduction in the signal intensity from both heterostructures, together with a similar shift in energy of the minority feature. The majority feature, instead, is quenched only for the Fe/Ni multilayer, which therefore presents a novel bulk band structure, possibly influencing also its electrical and magnetic response.

Several hypotheses can be proposed regarding the quenching of the in-plane spin polarization of the Ni buffer layer. Hybridization with O atoms is expected to produce changes in the electronic structure at the surface and hence a variation of the Ni and O magnetic moments [28]. However, given the reduced dimensionality of the system, this can also result in the rotation of the easy magnetization axis perpendicular to the (001) plane, as observed, *e.g.*, in the case of ultrathin *bcc* Fe films [29] or in the Ni/Cu(001) system [30] This occurrence cannot be captured by our experimental setup. Similarly, we are not sensitive to any possible antiferromagnetic ordering of the topmost layer, often characteristic of ultrathin transition metal oxide layers [13]. Upon the growth of the Fe overlayer and the restoration of the spin polarization in filled states, only the minority channel is restored in empty states. The result suggests that the growth of the Fe/Ni multilayer system onto Fe-*p*(1 × 1)O significantly modifies the majority bandstructure above the Fermi level. This could have important consequences (i) in the understanding of magnetic properties of confined metastable multilayers and (ii) in the field of spintronics for possible spin-engineered systems at the nanoscale.

Theoretical simulations have been therefore performed to better understand the quenching-restoration phenomena. We have performed simulations for: the Fe-*p*(1 × 1)O substrate; 1, 3, 6 and 12 Ni-*p*(1 × 1)O layers on Fe(001); 1, 3 and 6 Fe-*p*(1 × 1)O layers on top of 6 Ni layers on Fe(001). For simplicity, we present results here only for the Fe-*p*(1 × 1)O substrate (denoted as "substrate" in the following), O/6Ni/Fe ("6Ni") and O/1Fe/6Ni/Fe ("1Fe/6Ni"). Theoretical simulations on the other systems are reported in the Supporting Information.

In Table 1 we present the structural properties and the magnetic moment projected on the various atoms.

Table 1: Interlayer spacing and atomic magnetic moments at the surface of selected systems: the Fe-p(1×1)O substrate; 6 Ni-p(1×1)O layers on Fe(001); 1 Fe-p(1×1)O layer on 6 Ni/Fe(001). The computed Fe bulk interlayer spacing (=100%) amounts to 1.416 Å.

Substrate		6Ni		1Fe/6Ni	
Layers	Spacing (%)	Layers	Spacing (%)	Layers	Spacing (%)
O-Fe1	31.3	O-Ni1	16.6	O-Fe	31.7
Fe1-Fe2	115.5	Ni1-Ni2	118.9	Fe-Ni1	113.9
Fe2-Fe3	101.4	Ni2-Ni3	97.1	Ni1-Ni2	98.3
Atom	Magn. moment (μ_B)	Atom	Magn. moment (μ_B)	Atom	Magn. moment (μ_B)
O	0.27	O	0.10	O	0.34
Fe1	3.20	Ni1	0.21	Fe	3.38
Fe2	2.59	Ni2	0.65	Ni1	0.63
Fe3	2.40	Ni3	0.64	Ni2	0.60

Given its (1 × 1) symmetry, the multilayer structure can be characterized solely by considering the interlayer spacing. The Fe-*p*(1 × 1)O substrate, reported as a reference, shows a remarkable expansion of the first Fe-Fe interlayer spacing (Fe1-Fe2), by 15.5% in our calculations, with respect to the computed bulk distance of

1.416 Å and in agreement with the literature [31,32]. The distance between the O layer and Fe1 amounts to 31.3% of the bulk distance. For deposited Ni as in 6Ni, such O-surface distance is nearly halved to 16.6%, while the Ni1-Ni2 expands by 18.9%, so that the topmost Ni and O atoms form a single layer lift off the surface. Minor changes are seen in the layers below. For the 1 Fe/6 Ni system, a structure close to that of the first two layers (O, Fe1) of the *p*(1 × 1)O substrate is obtained.

Looking now to the magnetic structure, the presence of O enhances the spin-polarization of the Fe surface by about 0.8 μ_B with respect to the bulk value. Upon deposition of 6 layers of Ni (6Ni system), however, the surface magnetic moment becomes significantly smaller: 0.21 μ_B for the topmost Ni atoms, and about 0.5-0.6 μ_B for the subsurface ones. The strong reduction at the surface is due to binding to the O layer, since the value computed without O is 0.79 μ_B. Remarkably, as the 1Fe/6Ni system shows, adding one Fe layer is sufficient to restore the surface magnetization and indeed we find a larger value for the Fe atom than for Fe-*p*(1×1)O. Concurrently, the magnetization value for the topmost Ni layer under Fe is increased to 0.63 μ_B. In all these cases, a contribution to the surface spin polarization also comes from the regions surrounding the O atoms.

The changes in the spin polarization can be detailed by the analysis of the projected density of states for the same systems, reported in **Figure 5**.

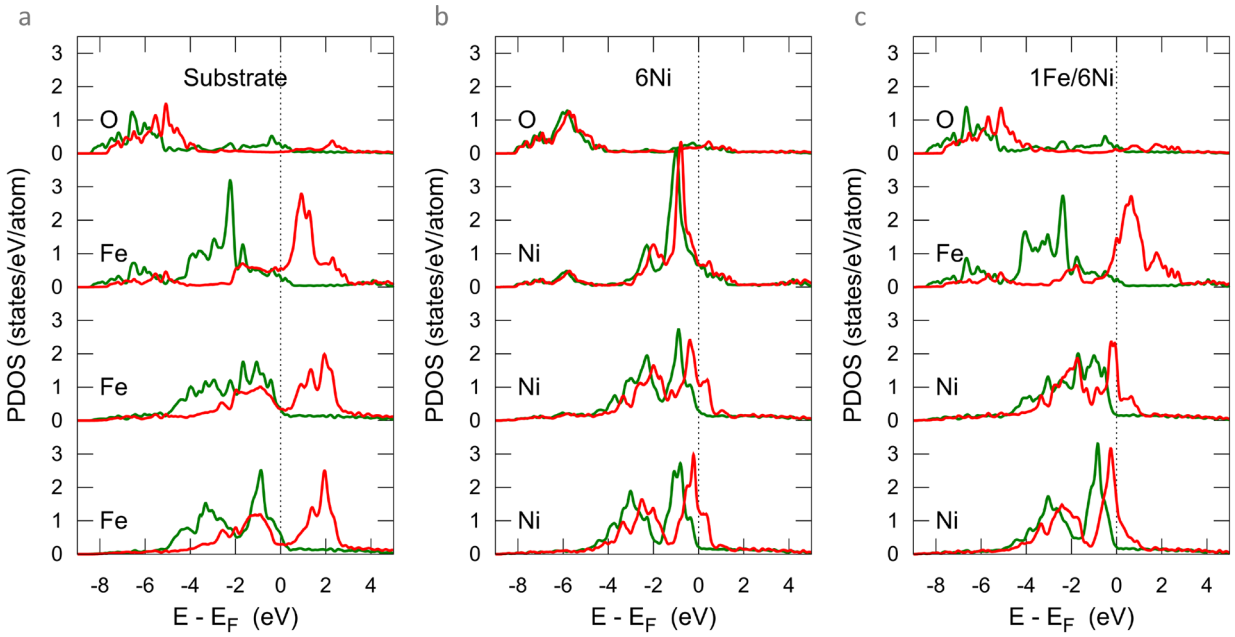

Figure 5: Partial Electronic Density Of States (PDOS) projected on the topmost four atomic layers for a) the Fe-p(1 × 1)O substrate b) 6 Ni-p(1 × 1)O layers on Fe(001) c) a Fe-p(1 × 1)O layer on 6 Ni/Fe(001). Green and red lines mark spin-majority and spin-minority states, respectively.

In all cases, the Partial Density of States (PDOS) of the first metal layer shows marked differences from the layers below. In the substrate (Figure 5a), also the second metal layer differs significantly from the deeper ones, whereas the PDOS of the third layer is similar to the bulk one (reported in the Supporting Information). The spin-majority *d*-states of Fe, that in the deep layers extend up to the unoccupied states, appear reduced around E_F. At higher energies, mostly *s-p* dispersing bands and spin-minority states are found, as also expected from many-body calculations of the bulk band structure [33] The reduced spin-polarization of the topmost Ni layer in the 6Ni system is clearly visible as the PDOS for the two spin components nearly overlap (Figure 5b). Comparing Figure 5c (1Fe/6Ni system) to Figure 5a (substrate), we can see that the PDOS of the topmost Fe layer is moderately influenced by the presence of Ni underneath, and a shift of Fe empty minority states towards the Fermi level, as a result of hybridization with Ni, can be observed. Conversely, all the Ni layers, excluding the topmost one in contact with Fe, exhibit a PDOS very similar to the one corresponding

to the 6 ML Ni case. Eventually, for thicker Fe overlayers grown on Ni (3 to 6 Fe layers on 6 Ni), the electronic and magnetic properties of the topmost Fe atoms closely match those of the Fe-*p*(1 × 1)O surface, as can be seen in the Supporting Information. States belonging to O atoms are found mainly in the energy range from -8 eV to -4 eV, with some spectral contributions close to the Fermi level as a result of hybridization with the underlying metal.

For a better comparison with our photoemission results, acquired at normal electron emission ($k_{\parallel} \lesssim 10^{-1}\text{Å}^{-1}$) [27], we have analysed the *k*-resolved PDOS, evaluated at the centre of the surface Brillouin zone ($k_{\parallel} = 0$). It includes also the k_z-dispersion, although this is sampled approximately, as the slab has a finite thickness. The results are shown in **Figure 6**.

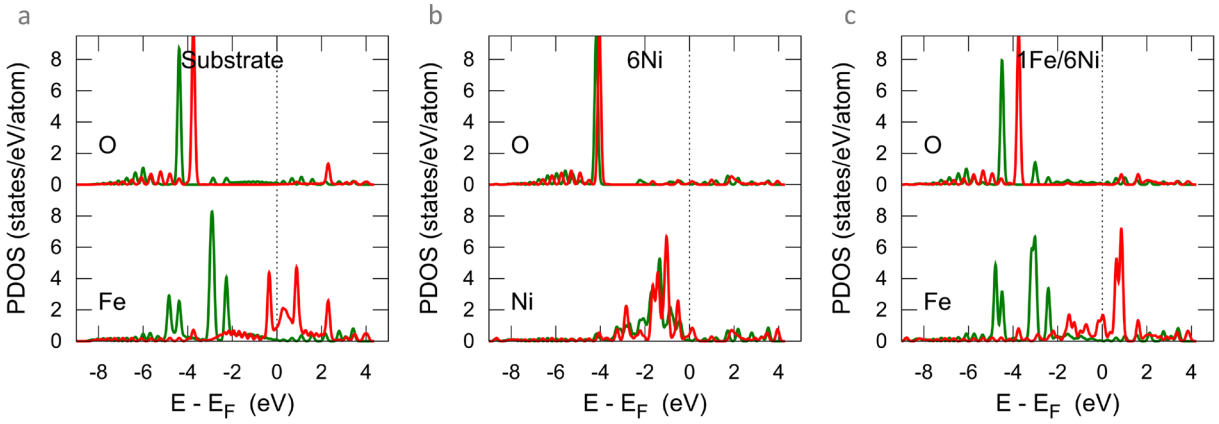

Figure 6: DFT electronic PDOS at the surface Γ point projected on the topmost two atomic layers for a) the Fe-p(1 × 1)O substrate b) 6 Ni-p(1 × 1)O layers on Fe(001) c) a Fe-p(1 × 1)O layer on 6 Ni/Fe(001). Green and red lines mark spin-majority and spin-minority states, respectively.

The sharp states that emerge from the O PDOS around -4 eV are due to in-plane *p* orbitals, as we found by resolving the PDOS in angular components (only the summary of the analysis is reported here). Such states are spin-split when O lies on a Fe layer (substrate and 1Fe/6Ni systems, shown in Figures 6a and 6c, respectively), due to the Fe-O interaction, and mostly independent from spin for the 6Ni case (figure 6b). An excellent agreement is found with the experimental results of Figure 3, region A (O 2*p* states), definitely proving that the quenching of the polarization signal in our experimental result is due to a reduction in the surface magnetization.

According to simulations, in the topmost Fe layer of the substrate, the two sharp peaks below -4 eV in the spin-majority states originate from $d_{x^2-y^2}$ and d_{zx}/d_{zy} orbitals. The structures at about -3 eV and -2 eV include Fe $d_{zx}/d_{zy}/d_{xy}$ and d_{z^2} contributions, respectively. Interestingly, the electronic structure of 1Fe/6Ni is very similar, with the same orbital assignments. Looking now to the empty states, we can see that in the range from the Fermi level to about 2 eV the electronic structure is dominated by spin-minority Fe states with *d*-character, while no such contributions are obtained for the Ni layers.

Simulations reveal only little differences between the electronic structure of the topmost substrate layer and that of 1 ML Fe on the Ni buffer layer, mostly due to the electronic interaction with the metallic layer immediately below. Consistently with this picture, these small differences vanish on thick Fe overlayers (see simulations for 3Fe/6Ni and 6Fe/6Ni in the Supporting Information), which indeed reproduce the same atomic structure of the substrate. An accurate comparison between our experimental results and the layer wise simulation of Fe and Ni electronic structure is not straightforward for those states characterized by a strong dispersion in the direction perpendicular to the surface, such as the empty majority feature C, that we assigned to photoemission from a bulk state. Nevertheless, it appears likely to us that the observed modifications in the Fe overlayer electronic structure have to be ascribed to a crystalline quality worsening or a structural relaxation of the overlayer, as already observed in homo- and hetero-epitaxial systems,

respectively [34,35], not captured by the simulations, rather than the effect of hybridization with the Ni buffer layer.

Conclusion

We have characterized the structural and magnetic properties of Fe/Ni multilayers growth on a Fe-*p*(1×1)O substrate by means of surface science techniques such as LEED, X-ray, and UV photoemission, complemented by DFT calculations. From the structural point of view, the XPS and LEED analyses confirm the growth of a commensurate *bcc* buffer layer with oxygen atoms in the first atomic layer. Spin-resolved photoemission results reveal a strong reduction of the spectral spin polarization. The subsequent deposition of a minimal amount of Fe (1 atomic layer) leads to an abrupt restoration of the pristine Fe-*p*(1 × 1)O surface and of the spin polarization in the band structure below the Fermi level. In addition, we observe a quenching of the majority electronic state above the Fermi energy. Simulations confirm that the magnetic moment of the topmost metal layer, enhanced by the presence of O for the Fe surface, is instead quenched when Ni is deposited. A single layer of Fe is sufficient to restore an even stronger magnetic moment of the topmost atoms.

Bibliography

[1] L. Häggström, I. Soroka, and S. Kamali, *Thickness Dependent Crystallographic Transition in Fe/Ni Multilayers*, Journal of Physics: Conference Series **217**, 012112 (2010).

[2] A. Frisk, H. Ali, P. Svedlindh, K. Leifer, G. Andersson, and T. Nyberg, *Composition, Structure and Magnetic Properties of Ultra-Thin Fe/Ni Multilayers Sputter Deposited on Epitaxial Cu/Si(001)*, Thin Solid Films **646**, 117 (2018).

[3] T. Kojima, M. Ogiwara, M. Mizuguchi, M. Kotsugi, T. Koganezawa, T. Ohtsuki, T.-Y. Tashiro, and K. Takanashi, *Fe–Ni Composition Dependence of Magnetic Anisotropy in Artificially Fabricated L1 0 -Ordered FeNi Films*, Journal of Physics: Condensed Matter **26**, 064207 (2014).

[4] C. S. Tian et al., *Body-Centered-Cubic Ni and Its Magnetic Properties*, Physical Review Letters **94**, 137210 (2005).

[5] N. B. Brookes, A. Clarke, and P. D. Johnson, *Electronic and Magnetic Structure of Bcc Nickel*, Physical Review B **46**, 237 (1992).

[6] A. Picone, A. Brambilla, A. Calloni, L. Duò, M. Finazzi, and F. Ciccacci, *Oxygen-Induced Effects on the Morphology of the Fe(001) Surface in out-of-Equilibrium Conditions*, Physical Review B **83**, 235402 (2011).

[7] A. Calloni, A. Picone, A. Brambilla, M. Finazzi, L. Duò, and F. Ciccacci, *Effects of Temperature on the Oxygen Aided Cr Growth on Fe(001)*, Surface Science **605**, 2092 (2011).

[8] J. Lindner, P. Poulopoulos, R. Nünthel, E. Kosubek, H. Wende, and K. Baberschke, *Improved Growth and the Spin Reorientation Transition of Ni on (√2×2√2)R45° Reconstructed O/Cu(001)*, Surface Science **523**, L65 (2003).

[9] A. Picone, M. Riva, A. Brambilla, A. Calloni, G. Bussetti, M. Finazzi, F. Ciccacci, and L. Duò, *Reactive Metal–Oxide Interfaces: A Microscopic View*, Surface Science Reports **71**, 32 (2016).

[10] A. Picone, G. Bussetti, M. Riva, A. Calloni, A. Brambilla, L. Duò, F. Ciccacci, and M. Finazzi, *Oxygen-Assisted Ni Growth on Fe(001): Observation of an "Anti-Surfactant" Effect*, Physical Review B **86**, 075465 (2012).

[11] A. Picone, M. Riva, G. Fratesi, A. Brambilla, G. Bussetti, M. Finazzi, L. Duò, and F. Ciccacci, *Enhanced Atom Mobility on the Surface of a Metastable Film*, Physical Review Letters **113**, 046102 (2014).

[12] R. Bertacco and F. Ciccacci, *Oxygen-Induced Enhancement of the Spin-Dependent Effects in Electron Spectroscopies of Fe(001)*, Physical Review B **59**, 4207 (1999).

[13] G. Berti, A. Brambilla, A. Calloni, G. Bussetti, M. Finazzi, L. Duò, and F. Ciccacci, *Oxygen-Induced Immediate Onset of the Antiferromagnetic Stacking in Thin Cr Films on Fe(001)*, Applied Physics Letters **106**, 162408 (2015).

[14] G. Berti, A. Calloni, A. Brambilla, G. Bussetti, L. Duò, and F. Ciccacci, *Direct Observation of Spin-Resolved Full and Empty Electron States in Ferromagnetic Surfaces*, Review of Scientific Instruments **85**, 073901 (2014).

[15] G. Bussetti, M. Riva, A. Picone, A. Brambilla, L. Duò, M. Finazzi, and F. Ciccacci, *Martensitic Transition during Ni Growth on Fe(001): Evidence of a Precursor Phase*, New Journal of Physics **14**, 053048 (2012).

[16] G. C. Burnett, T. J. Monroe, and F. B. Dunning, *High-efficiency Retarding-potential Mott Polarization Analyzer*, Review of Scientific Instruments **65**, 1893 (1994).

[17] J. P. Perdew, K. Burke, and M. Ernzerhof, *Generalized Gradient Approximation Made Simple*, Physical Review Letters **77**, 3865 (1996).

[18] P. Giannozzi et al., *QUANTUM ESPRESSO: A Modular and Open-Source Software Project for Quantum Simulations of Materials*, Journal of Physics: Condensed Matter **21**, 395502 (2009).

[19] P. Giannozzi et al., *Advanced Capabilities for Materials Modelling with Quantum ESPRESSO*, Journal of Physics: Condensed Matter **29**, 465901 (2017).

[20] A. Picone, G. Fratesi, M. Riva, G. Bussetti, A. Calloni, A. Brambilla, M. I. Trioni, L. Duò, F. Ciccacci, and M. Finazzi, *Self-Organized Chromium Oxide Monolayers on Fe(001)*, Physical Review B **87**, 085403 (2013).

[21] A. v. Naumkin, A. Kraut-Vass, S. W. Gaarenstroom, and C. J. Powell, *NIST X-Ray Photoelectron Spectroscopy Database*, https://doi.org/10.18434/T4T88K.

[22] A. P. Grosvenor, M. C. Biesinger, R. St. C. Smart, and N. S. McIntyre, *New Interpretations of XPS Spectra of Nickel Metal and Oxides*, Surface Science **600**, 1771 (2006).

[23] L. Gragnaniello, F. Allegretti, R. R. Zhan, E. Vesselli, A. Baraldi, G. Comelli, S. Surnev, and F. P. Netzer, *Surface Structure of Nickel Oxide Layers on a Rh(111) Surface*, Surface Science **611**, 86 (2013).

[24] S. Tanuma, C. J. Powell, and D. R. Penn, *Calculation of Electron Inelastic Mean Free Paths (IMFPs) VII. Reliability of the TPP-2M IMFP Predictive Equation*, Surface and Interface Analysis **35**, 268 (2003).

[25] A. Cattoni, D. Petti, S. Brivio, M. Cantoni, R. Bertacco, and F. Ciccacci, *MgO/Fe(001) and MgO/Fe(001)−p(1×1)O*, Physical Review B **80**, 104437 (2009).

[26] G. Gewinner, J. C. Peruchetti, and A. Jaéglé, *Ordered Oxygen Overlayers on Cr(100) Observed by Leed and Photoemission*, Surface Science **122**, 383 (1982).

[27] A. Calloni, G. Fratesi, S. Achilli, G. Berti, G. Bussetti, A. Picone, A. Brambilla, P. Folegati, F. Ciccacci, and L. Duò, *Combined Spectroscopic and Ab Initio Investigation of Monolayer-Range Cr Oxides on Fe(001): The Effect of Ordered Vacancy Superstructure*, Physical Review B **96**, 085427 (2017).

[28] Y. Murata, S. Ohtani, and K. Terada, *Electronic Energy Levels Induced by Chemisorbed Oxygen on the (100) Plane of Nickel*, Japanese Journal of Applied Physics **13**, 837 (1974).

[29] B. Heinrich, J. F. Cochran, A. S. Arrott, S. T. Purcell, K. B. Urquhart, J. R. Dutcher, and W. F. Egelhoff, *Development of Magnetic Anisotropies in Ultrathin Epitaxial Films of Fe(001) and Ni(001)*, Applied Physics A Solids and Surfaces **49**, 473 (1989).

[30] J. Hong, R. Q. Wu, J. Lindner, E. Kosubek, and K. Baberschke, *Manipulation of Spin Reorientation Transition by Oxygen Surfactant Growth: A Combined Theoretical and Experimental Approach*, Physical Review Letters **92**, 147202 (2004).

[31] P. Błoński, A. Kiejna, and J. Hafner, *Theoretical Study of Oxygen Adsorption at the Fe(110) and (100) Surfaces*, Surface Science **590**, 88 (2005).

[32] A. Picone et al., *Atomic Corrugation in Scanning Tunneling Microscopy Images of the Fe(001)–p(1×1)O Surface*, Physical Review B **81**, 115450 (2010).

[33] A. Yamasaki and T. Fujiwara, *Electronic Structure of Transition Metals Fe, Ni and Cu in the* G W *Approximation*, Journal of the Physical Society of Japan **72**, 607 (2003).

[34] F. Ciccacci and S. de Rossi, *Empty Electronic States in Magnetic Thin Films: Fe on Au(100), Ag(100), and Cu(100)*, Physical Review B **51**, 11538 (1995).

[35] A. Calloni, G. Berti, G. Bussetti, G. Fratesi, M. Finazzi, F. Ciccacci, and L. Duò, *Electronic Structure and Magnetism of Strained Bcc Phases across the Fcc to Bcc Transition in Ultrathin Fe Films*, Physical Review B **94**, 195155 (2016).